We 21 B11

Rapid Inversion of Data from 2-D and from 3-D Resistivity Surveys with Shifted Electrodes

M.H. Loke* (Geotomo Software Pty Ltd), P.B. Wilkinson (British Geological Survey) & J.E. Chambers (British Geological Survey)

SUMMARY

Geoelectrical monitoring surveys are used to detect temporal changes in the subsurface below unstable slopes with the measurements repeated over an extended period. The positions of the electrodes are measured at the start of the campaign and possibly at regular intervals. However, ground movements sometimes occur between the times of the electrode positions measurements. For some data sets the precise positions of the electrodes are not accurately known and have to be estimated from the resistivity data. The smoothness-constrained least-squares optimization method is modified to include the electrode positions as unknown parameters to be determined. The Jacobian matrices with the sensitivity of the apparent resistivity measurements to changes in the electrode positions are required by the optimization method. A fast adjoint-equation method to calculate the required Jacobian matrices is described. It is one to two orders of magnitude faster than the perturbation method previously used. We also modify the inversion routine by using the inversion model for the initial time-lapse data set (with known electrode positions) as the starting model for the inversion of the later-time data sets. This greatly improves the accuracy of the recovered electrode positions compared to the use of a homogeneous earth starting model.

Introduction

2-D and 3-D resistivity surveys are now widely used in archaeological, hydrology, geotechnical, environmental and mineral exploration problems (Loke *et al.*, 2011). Geoelectrical monitoring surveys are used to detect temporal changes in the subsurface (Supper *et al.*, 2014), such as the monitoring of unstable slopes. The measurements are repeated a number of times. The electrode positions are measured at the start of the campaign and possibly also at regular intervals. However, ground movements sometimes occur between the times of electrode positions measurements. Also the electrode positions might not be accurately known for some data sets. Thus is necessary to determine the shifts in the electrode positions from the resistivity data itself (Wilkinson *et al.*, 2015). A method was presented by Kim (2014) where both the subsurface resistivity and electrodes positions are unknown variables to be determined by the least-squares optimization method. In this paper, we present a rapid method to determine the required Jacobian matrix of partial derivatives. We also modify the inversion algorithm to use the inversion model from a previous time-lapse data set to improve the accuracy of the estimated electrode positions.

Method

(a) A modification to the constrained least-squares optimization method

The smoothness-constrained least-squares optimization method is frequently used for 2-D and 3-D inversion of resistivity data. The modified least-squares equation (Kim, 2014) where the electrode positions are included as unknown variables may be written as

$$\left[\mathbf{G}_\mathbf{i}^\mathbf{T}\mathbf{R}_\mathbf{d}\mathbf{G}_\mathbf{i} + \boldsymbol{\lambda}_\mathbf{i}\mathbf{V}^\mathbf{T}\mathbf{R}_\mathbf{m}\mathbf{V}\right]\Delta\mathbf{q}_\mathbf{i} = \mathbf{G}_\mathbf{i}^\mathbf{T}\mathbf{R}_\mathbf{d}\mathbf{g}_\mathbf{i} - \boldsymbol{\lambda}_\mathbf{i}\mathbf{V}^\mathbf{T}\mathbf{R}_\mathbf{m}\mathbf{V}\,\mathbf{q}_{\mathbf{i-1}} \qquad (1)$$

where

$$\mathbf{q} = \begin{pmatrix}\mathbf{r}\\ \mathbf{x}\\ \mathbf{z}\end{pmatrix}, \mathbf{G} = \begin{pmatrix}\mathbf{J}\\ \mathbf{X}\\ \mathbf{Z}\end{pmatrix}, \mathbf{V} = \begin{pmatrix}\mathbf{W}\\ \alpha\mathbf{W}_\mathbf{x}\\ \beta\mathbf{W}_\mathbf{y}\end{pmatrix}.$$

The combined Jacobian matrix **G** consists of **J** (the model resistivity sensitivity values), **X** and **Z** (the sensitivity values for the changes in the *x* and *z* electrode positions) matrices. $\boldsymbol{\lambda}$ is a damping factor vector and **g** is the data misfit vector. **q** is the model parameters vector consisting of **r** (model resistivity) and **x** and **z** (electrode position) vectors. $\Delta\mathbf{q}_\mathbf{i}$ is the change in the model parameters. **W** is the resistivity spatial roughness filter term. $\mathbf{W}_\mathbf{x}$ and $\mathbf{W}_\mathbf{y}$ are the roughness filters for the electrode position vectors. $\mathbf{R}_\mathbf{d}$ and $\mathbf{R}_\mathbf{m}$ are weighting matrices used by the L1-norm inversion method (Loke *et al.*, 2003). α and β are the relative damping factor weights for the shifts in the electrode positions. A homogeneous half space is commonly used as the starting model for the optimization algorithm. In a time-lapse survey the initial positions of the electrodes are usually accurately measured, and can be treated as fixed parameters in the inversion of the initial data set. The temporal changes in the subsurface resistivity are usually much less than the spatial variations (Loke *et al*, 2014). Thus the inversion model of the initial data set provides a good starting model for the later time data sets. We modify the inversion algorithm to use the model from a previous survey as the starting model.

(b) A fast method to calculate the Jacobian matrix using the finite-element method

The potentials are calculated by solving the following finite-element capacitance matrix equation.

$$\mathbf{C}\boldsymbol{\Phi} = \mathbf{s} \qquad (2)$$

$\boldsymbol{\Phi}$ is a vector with the potentials at the nodes of the mesh while **s** is the current source vector. **C** is the capacitance matrix that contains the positions of the nodes and model conductivity values. The **C** matrix is a symmetric sparse matrix with 9 non-zero sub-diagonals for 2-D linear quadrilateral elements (27 for 3-D hexahedral elements). Kim (2014) used the perturbation method to calculate the necessary partial derivatives for changes in the electrode positions. For example, a change in the *x*-position of electrode number 2 is approximated by

$$\frac{\partial\phi_i}{\partial x_2} \approx \frac{\phi_i(x_2+\Delta x_2)-\phi_i(x_2)}{\Delta x_2}. \qquad (3)$$

For a survey line with e electrodes it will be necessary to calculate the potentials by resolving equation (2) $2e$ times. While this is possible for 2-D problems, it becomes impractical for 3-D problems where the forward modeling routine is about two to three orders of magnitude slower. Furthermore, it is necessary to calculate the partial derivatives in 3 directions (x, y, z). We describe a modification of the adjoint-equation approach (McGillivray and Oldenburg, 1990) to calculate the **X** and **Z** Jacobian matrices. For example, by differentiating equation (2) with respect to z_k, the derivative of the potential values ($\partial\mathbf{\Phi}/\partial z_k$) due to a shift in the z direction for the kth electrode is as follows.

$$\mathbf{C}\frac{\partial\mathbf{\Phi}}{\partial z_k} = -\frac{\partial\mathbf{C}}{\partial z_k}\mathbf{\Phi} \tag{5}$$

It is only necessary to calculate the non-zero terms in the $\partial\mathbf{C}/\partial z_k$ matrix as this equation has the same form as (2). Figure 1 shows part of the 2-D finite-element mesh. A shift in the position of one electrode (3) will only affect the nodes that lie between the adjacent electrodes (2 to 4). Thus the $\partial\mathbf{C}/\partial z_k$ matrix has a relatively small number of non-zero terms compared to the full **C** matrix. The elements of the **C** matrix have the following form (Silvester and Ferrari, 1990).

$$c_{pq} = k_{pq}(x,z)\ \sigma_j \tag{6}$$

where σ_j is the model cell conductivity. The function $k_{pq}(x,z)$ depends only on the coordinates of the nodes at the corners of the quadrilateral element. The change in the coupling coefficients are calculated numerically using a two-sided finite-difference formula as follows.

$$\frac{\partial c_{pq}}{\partial z_k} \approx \frac{k_{pq}(x, z_k + \Delta z_k) - k_{pq}(x, z_k - \Delta z_k)}{2\Delta z_k}\sigma_j \tag{7}$$

The two-sided formula avoids the directional bias in a one-sided formula such as (3). The time required to calculate the $k_{pq}(x,z)$ terms is negligible compared to resolving equation (2) as required by the perturbation method. The partial derivative vector $\partial\mathbf{\Phi}/\partial z_k$ values are calculated by multiplying the non-zero elements in the $\partial\mathbf{C}/\partial z_k$ matrix by the net potentials at the nodes due to current sources at the positions of the current electrodes used in the measurement. The resulting vector is then multiplied by the net potentials at the nodes due to current sources at the positions of the potential electrodes. The required potentials are already available in the process of solving (2) to calculate the apparent resistivity values. For a 2-D survey line with 50 electrodes, it is estimated that the adjoint-equation method is about 44 times faster than the perturbation method.

Results

Figure 2a shows a synthetic model below a survey line with 31 electrodes with a uniform 1 m spacing on a flat surface. Figure 2b shows the perturbed model with four changes. The electrode at the 5.0 m mark is shifted 0.3 m. to the right. The electrode at the 17.0 m mark is shifted 0.4 m. upwards. A 70 ohm.m prism (depth of 1.0 m to the top) is added between the two existing prisms, and the 20 ohm.m low resistivity prism is extended downwards by 0.73 m. The measured data consists of dipole-dipole arrays with the '*a*' dipole lengths ranging from 1 to 4 m., and the '*n*' factor ranging from 1 to 6. This gives a total of 415 data points. Gaussian random noise (Zhou and Dahlin, 2003) with a mean amplitude of 2.5 milliohm was added to the data before they were converted to apparent resistivity values. The average noise level for the data set is about 1.0%. Figure 2 shows the inversion models obtained assuming the electrodes are equally spaced on a flat surface. The model for the perturbed data set has significant distortions (Figure 2b). We next carry out an inversion of the perturbed data set using a homogeneous half space as the starting model. Initially the electrodes equally spaced but they are allowed to shift during the inversion process. Figure 3 shows the models obtained using different values for the relative damping factor weights (α and β) ranging from 1 to 100. The three subsurface prisms are well resolved. The upwards spike of the surface at the 17 m mark is clearly shown. However, there is a distortion in the surface profile over the high resistivity prism. This is more clearly shown in the profile plots in Figure 4a. The inversion algorithm is not able to fully distinguish between the effects of vertical shifts in the electrodes and an increase in the shallow subsurface resistivity. The distortion of the surface profile is progressively reduced when the damping factor is increased, and almost completely eliminated with a relative damping factor of 100.0 (Kim, 2014). However, increasing the higher damping factor also decreases the spike in the elevation at the electrode located at the 17 m. mark. Figure 5 shows the inversion results for the perturbed data set when the inversion model for the initial data set (Figure 2a) is used as the starting model. The distortions in the surface profile over the high resistivity block are eliminated. The most accurate results are obtained with the smallest relative damping factor of 1.0 (Figures 4b).

Conclusions

A fast technique to calculate the Jacobian matrix values for shifts in the electrode positions using the adjoint-equation method is presented. The use of the inversion model for the initial data set (with known electrode positions) as the starting model for a later data set eliminates the distortions in the profile caused by subsurface resistivity variations giving more accurate calculated electrode positions.

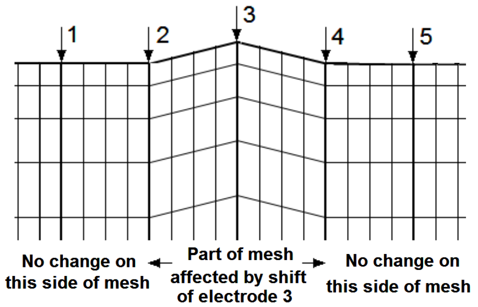

Figure 1 *The parts of a 2-D finite-element mesh affected by a shift in the position of electrode 3.*

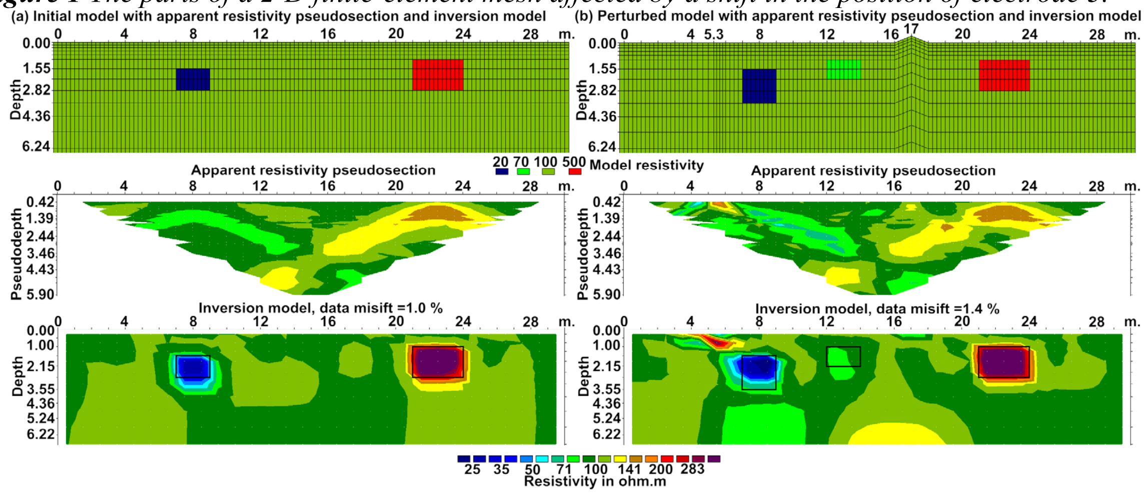

Figure 2 *The (a) initial and (b) perturbed synthetic test models with apparent resistivity pseudosections and inversion models assuming a constant electrode spacing and flat surface.*

References

Kim, J.H. [2014] Simultaneous Inversion of Resistivity Structure and Electrode Locations in ERT. *20th European Meeting of Environmental and Engineering Geophysics*, Athens, Greece, 14-18 September 2014, We Olym 10.

Loke, M.H., Acworth, I. and Dahlin, T. [2003] A comparison of smooth and blocky inversion methods in 2D electrical imaging surveys. *Exploration Geophysics*, **34**, 182-187.

Loke, M.H., Chambers, J.E., Rucker, D.F., Kuras, O. and Wilkinson, P.B. [2013] Recent developments in the direct-current geoelectrical imaging method. *Journal of Applied Geophysics*, **95**, 135-156.

Loke, M.H., Dahlin, T., Rucker, D.F. [2014] Smoothness-constrained time-lapse inversion of data from 3-D resistivity surveys. *Near Surface Geophysics*, **12**, 5-24.

McGillivray, P.R. and Oldenburg, D.W. [1990] Methods for calculating fréchet derivatives and sensitivities for the non-linear inverse problem: a comparative study. *Geophysical Prospecting*, **38**,499-524.

Silvester, P.P. and Ferrari, R.L. [1990] *Finite elements for electrical engineers (2nd. ed.)*. Cambridge University Press.

Supper, R., Ottowitz, D., Jochum, B., Römer, A., Pfeiler, S., Kauer, S., Keuschnig, M. and Ita, A. [2014] Geoelectrical monitoring of frozen ground and permafrost in alpine areas: field studies and considerations towards an improved measuring technology. *Near Surface Geophysics*, **12**, 93-115.

Wilkinson, P.B., Uhlemann, S., Chambers, J.C., Meldrum, P. I. and Loke, M.H. [2015] Development and testing of displacement inversion to track electrode movements on 3D Electrical Resistivity Tomography monitoring grids. *Geophysical Journal International*, **200**, 1566-1581.

Zhou, B. and Dahlin, T. [2003] Properties and effects of measurement errors on 2D resistivity imaging surveying. *Near Surface Geophysics*, **1**, 105-117.

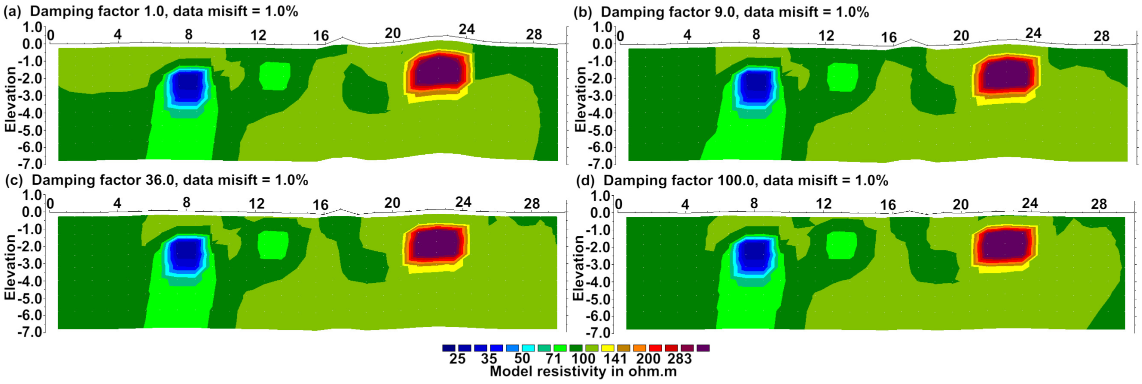

Figure 3 *The inversion models for the perturbed data set using different relative damping factors for the x and z coordinates of the electrodes, and a homogenous half space starting resistivity model.*

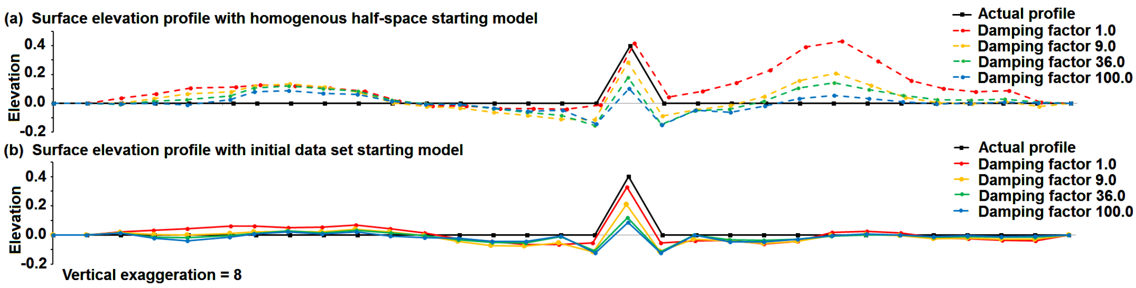

Figure 4 *The surface elevation profiles obtained using (a) a homogeneous half-space and (b) the inversion model of the initial time-lapse data set as the starting model for the inversion routine.*

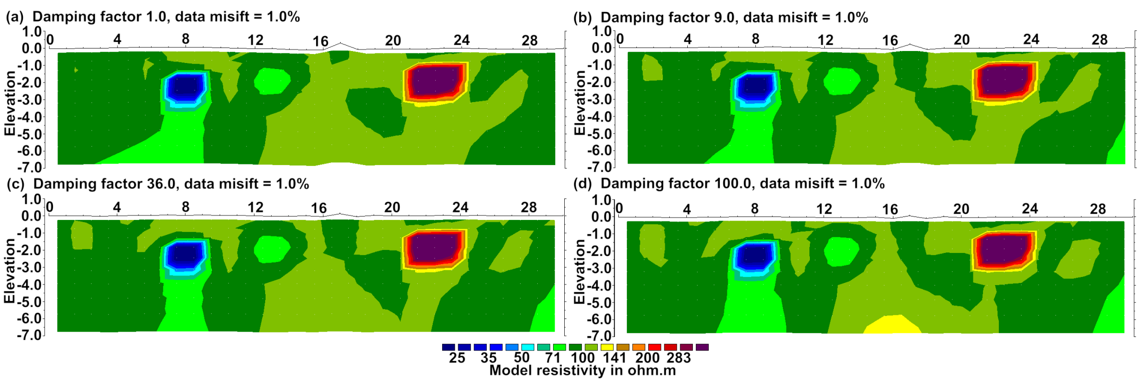

Figure 5 *The inversion models for the second time-lapse data set using different relative damping factors for the x and z coordinates of the electrodes. The model obtained from the inversion of the first time-lapse data set was used as the starting resistivity model.*